Missile Longitudinal Autopilots: Connections Between Optimal Control and Classical Topologies

Curtis P. Mracek * and D. Brett Ridgely †

Raytheon Missile Systems, Tucson, AZ 85734, USA

For several decades classical three loop autopilot topologies have been successfully employed as missile longitudinal autopilots. This paper deals with the autopilot design process from an optimal control perspective. The optimal control solution of the weighted sum of acceleration error and control usage results in a two loop topology. The weighted sum of acceleration error and control rate results in a three loop topology. A state transformation that leads to the "classic" autopilot[1] is presented. This paper then introduces what is termed a "neoclassic" topology. This topology adds a fourth loop so that "all" rate and acceleration gains are used. The four loop topology uses the same plant model as the three loop autopilots except that an added first order lag (which can represent additional dynamics, such as a Control Actuation System (CAS)) is explicitly taken into account using the additional gain. The four loop design reduces to the "classic" three loop topology as the lag bandwidth becomes infinite. Two five loop topology are also introduced which may be useful but one does not reduce to the superior robustness case as the CAS bandwidth is increased.

I. Introduction

Longitudinal autopilots for tactical missiles have been successfully employed for over fifty years. In the past several years, at Raytheon, the "classic" three loop autopilot (often dubbed the "Raytheon autopilot"[1]) has been the design topology of choice. The design goal of any autopilot is to use sensed quantities to produce a stable response that robustly follows commanded inputs. The classic three loop autopilot has the desired longitudinal acceleration as the command and the sensed acceleration and sensed angular rate as the measured quantities. This paper deals with approaching the autopilot design process by looking at the optimal control problem. It is found that solving the optimal control problem where the cost is a weighted sum of the acceleration error and the fin deflection leads to a two loop controller. The optimal control problem where the cost is the weighted sum of the acceleration error and the fin rates leads to a three loop topology. Next, a "neoclassic" four loop autopilot is presented that has the same commanded and sensed quantities as the three loop designs, but uses four gains instead of three. The adaptation for a Linear Quadratic (LQ) design technique is developed which allows for the direct augmentation of a first order dynamics model (to represent the CAS, IMU, delays, etc.) to the plant. Two five loop topologies are also introduced which allows augmentation of a second order dynamics model to the system. The five loop design requires either more than a single integration of the commanded acceleration or a first order lead. All higher order designs result in either double integration of the acceleration command or the four loop design with more and more complex lead systems. A longitudinal missile example is used throughout the paper to clarify the discussion.

II. Missile Longitudinal Dynamics

A missile's longitudinal dynamics can be described using the short period approximation of the longitudinal equations of motion. Written in state space notation the basic missile longitudinal plant is

$$\begin{aligned} \dot{x} &= Ax + Bu \\ y &= Cx + Du \end{aligned} \tag{1}$$

*Engineering Fellow, Raytheon Missile Systems, Senior Member AIAA

†Senior Department Manager, Raytheon Missile Systems, Senior Member AIAA

where

$$x = \begin{bmatrix} \alpha \\ q \end{bmatrix} \qquad u = \delta_p \qquad y = \begin{bmatrix} A_{z_m} \\ q_m \end{bmatrix}$$

To be more specific, the short period dynamics are

$$A = \begin{bmatrix} \frac{1}{V_{m_0}} \left[\frac{\bar{Q}SC_{z\alpha_0}}{m} - A_{X_0} \right] & 1 \\ \frac{\bar{Q}SdC_{m\alpha_0}}{I_{YY}} & 0 \end{bmatrix} \qquad B = \begin{bmatrix} \frac{\bar{Q}SC_{z\delta_{p_0}}}{mV_{m_0}} \\ \frac{\bar{Q}SdC_{m\delta_{p_0}}}{I_{YY}} \end{bmatrix}$$

$$C = \begin{bmatrix} \frac{\bar{Q}SC_{z\alpha_0}}{mg} - \frac{\bar{Q}SdC_{m\alpha_0}\bar{x}}{gI_{YY}} & 0 \\ 0 & 1 \end{bmatrix} \qquad D = \begin{bmatrix} \frac{\bar{Q}SC_{z\delta_{p_0}}}{mg} - \frac{\bar{Q}SdC_{m\delta_{p_0}}\bar{x}}{gI_{YY}} \\ 0 \end{bmatrix}$$

The following numerical values will be used in the examples throughout this paper. Note that when $C_{m\alpha_0}$ is positive, the system is statically unstable, and stable when $C_{m\alpha_0}$ is negative.

Variable	Value	Units	Description
V_{m_0}	3350	ft/sec	Total Missile Velocity
m	11.1	slug	Total Missile Mass
I_{YY}	137.8	slug-ft^2	Pitch Moment of Inertia
$\bar{x}$	1.2	ft	Distance from CG to IMU Positive Forward
A_{X_0}	-60	ft/sec^2	Axial Acceleration Positive Forward
$C_{z\alpha_0}$	-5.5313	-	Pitch Force Coefficient due to Angle of Attack
$C_{m\alpha_0}$	±6.6013	-	Pitch Moment Coefficient due to Angle of Attack
$C_{z\delta_{p_0}}$	-1.2713	-	Pitch Force Coefficient due to Fin Deflection
$C_{m\delta_{p_0}}$	-7.5368	-	Pitch Moment Coefficient due to Fin Deflection
$\bar{Q}$	13332	lb/ft^2	Dynamic Pressure
S	0.5454	ft^2	Reference Area
d	0.8333	ft	Reference Length
g	32.174	ft/sec^2	Gravity Constant

For the unstable system this yields

$$A = \begin{bmatrix} -1.064 & 1 \\ 290.26 & 0 \end{bmatrix} \qquad B = \begin{bmatrix} -0.25 \\ -331.40 \end{bmatrix}$$

$$C = \begin{bmatrix} -123.34 & 0 \\ 0 & 1 \end{bmatrix} \qquad D = \begin{bmatrix} -13.51 \\ 0 \end{bmatrix}$$

and the open loop transfer functions are

$$\frac{A_{z_m}}{\delta_p} = \frac{-13.51s^2 + 16.29s + 44800}{s^2 + 1.064s - 290.26} = \frac{-13.51(s + 56.98)(s - 58.18)}{(s + 17.58)(s - 16.51)}$$

and

$$\frac{q_m}{\delta_p} = \frac{-331.4s - 424.7}{s^2 + 1.06s - 290.28} = \frac{-331.4(s + 1.281)}{(s + 17.58)(s - 16.51)}$$

This plant is a relatively fast unstable missile.

For the stable system the state space description is given by

$$A = \begin{bmatrix} -1.064 & 1 \\ -290.26 & 0 \end{bmatrix} \qquad B = \begin{bmatrix} -0.25 \\ -331.39 \end{bmatrix}$$

$$C = \begin{bmatrix} -101.71 & 0 \\ 0 & 1 \end{bmatrix} \qquad D = \begin{bmatrix} -13.51 \\ 0 \end{bmatrix}$$

and the open loop transfer functions are

$$\frac{A_{z_m}}{\delta_p} = \frac{-13.51s^2 + 10.91s + 29780}{s^2 + 1.064s + 290.26} = \frac{-13.51(s + 46.55)(s - 47.35)}{(s + 0.53 \pm 17.03j)}$$

and

$$\frac{q_m}{\delta_p} = \frac{-331.4s - 280.3}{s^2 + 1.064s + 290.26} = \frac{-331.4(s + 0.846)}{(s + 0.53 \pm 17.03j)}$$

This plant is a relatively fast lightly damped stable missile. Both of these models conform to the sign convention that a positive pitch fin deflection produces a negative moment.

III. Autopilot Development as an Optimal Control Problem

In this section, the design of the pitch autopilot will be set up as an LQR optimal control problem. Several extensions to the "standard" LQR problem are required here, including feedforward terms in the objective, output feedback, and tracking a step command. These will all be dealt with in the following subsections. As a quick refresher and to establish notation, the "standard" LQR problem is[4]

$$\min_u J = \int_0^\infty \left(z^T Q z + u^T R u \right) \, \mathrm{d}t$$

subject to the dynamics

$$\begin{aligned} \dot{x} &= Ax + Bu \\ z &= Hx \end{aligned}$$

with (A, B) stabilizable, (H, A) detectable, $Q \geq 0$ and $R > 0$. The optimal state feedback is given by

$$u = Kx$$

where

$$K = -R^{-1} B^T P$$

and P is the positive semidefinite stabilizing solution to the algebraic Riccati equation

$$0 = A^T P + PA - PBR^{-1} B^T P + H^T Q H$$

A. LQ State Feedback with Feedthrough Term in Objective

The solution of the linear quadratic optimal control problem with a feedthrough term in the optimization objective is derived in this section. The optimization objective is given as

$$\begin{aligned} \min_u J &= \int_0^\infty \left(z^T \tilde{Q} z + u^T \tilde{R} u \right) \, \mathrm{d}t \\ \text{s.t.} \quad \dot{x} &= Ax + Bu \\ z &= Hx + Lu \end{aligned}$$

Substituting z into the performance index yields

$$\min_u J = \int_0^\infty \left[(Hx + Lu)^T \tilde{Q} (Hx + Lu) + u^T \tilde{R} u \right] \, \mathrm{d}t$$

Let

$$\begin{aligned} Q &= H^T \tilde{Q} H \\ S &= H^T \tilde{Q} L \\ R &= \tilde{R} + L^T \tilde{Q} L \end{aligned}$$

then the performance index becomes

$$\min_u J = \int_0^\infty \left(x^T Q x + x^T S u + u^T S^T x + u^T R u \right) \, dt$$

This optimal control problem can be solved by forming the Hamiltonian

$$\mathcal{H} = x^T Q x + x^T S u + u^T S^T x + u^T R u + \left(\frac{\partial J^*}{\partial x} \right)^T [Ax + Bu]$$

Taking the partial of the Hamiltonian with respect to the control and setting this to zero. This results in

$$\frac{\partial \mathcal{H}}{\partial u} = 2S^T x + 2Ru + B^T \left(\frac{\partial J^*}{\partial x} \right) = 0$$

so that

$$u^* = -R^{-1} \left[\frac{1}{2} B^T \left(\frac{\partial J^*}{\partial x} \right) + S^T x \right]$$

The Hamilton-Jacobi equation then becomes

$$\begin{aligned} -\frac{\partial J^*}{\partial t} &= \mathcal{H}^* = x^T \left(Q - S R^{-1} S^T \right) x + \left(\frac{\partial J^*}{\partial x} \right)^T Ax \\ &\quad -\frac{1}{4} \left(\frac{\partial J^*}{\partial x} \right)^T B R^{-1} B^T \left(\frac{\partial J^*}{\partial x} \right) - x^T S R^{-1} B^T \left(\frac{\partial J^*}{\partial x} \right) \end{aligned}$$

Assume the optimal performance index has the form

$$J^* = x^T P x$$

so that

$$\frac{\partial J^*}{\partial t} = x^T \dot{P} x \qquad \frac{\partial J^*}{\partial x} = 2Px$$

Substituting these in the Hamilton-Jacobi equation and rearranging terms we get

$$-x^T \dot{P} x = x^T \left[(A - BR^{-1}S^T)^T P + P(A - BR^{-1}S^T) - PBR^{-1}B^T P + \left(Q - SR^{-1}S^T \right) \right] x$$

Since this is an infinite horizon problem, it is easy to show that $\dot{P} \longrightarrow 0$, so that we have the algebraic Riccati equation

$$(A - BR^{-1}S^T)^T P + P(A - BR^{-1}S^T) - PBR^{-1}B^T P + \left(Q - SR^{-1}S^T \right) = 0 \tag{2}$$

where we also require that

$$Q - SR^{-1}S^T \geq 0$$

and the optimal control is given by

$$u^* = Kx = -R^{-1} \left(B^T P + S^T \right) x$$

where P is the stabilizing solution of Equation 2.

B. Optimal Solution with Full State Observability

Next we will deal with the problem that the full state is not available for feedback in a missile control problem. Define "full state observability" as requiring that C^{-1} and $\left[I + KC^{-1}D\right]^{-1}$ exist. Then any state feedback optimal solution can be transformed to output feedback given the system is full state observable. That is, given the state feedback solution

$$u = Kx$$

and the output relation

$$y = Cx + Du$$

with C^{-1} existing, it is easy to see that

$$x = C^{-1}\left(y - Du\right)$$

The optimal control is then

$$u = KC^{-1}\left(y - Du\right)$$

Solving for the control using the assumption that $\left[I + KC^{-1}D\right]^{-1}$ exists results in

$$u = \left[I + KC^{-1}D\right]^{-1} KC^{-1}y$$

which is now an output feedback law. Clearly, if $D = 0$, the requirement to transform a state feedback solution to output feedback reduces to requiring C^{-1} to exist, as this becomes a state transformation.

C. Regulator Problem

The autopilot, at its most basic, is trying to control the airframe while regulating/tracking an acceleration. So let's try to set up an optimization problem to find the "best" control. We will begin with the regulation problem. The obvious optimization objective would be to use a weighted sum of the measured acceleration and the control usage. If there is no penalty on control usage the optimal controller would be bang-bang or singular control. A reasonable cost would thus be something like

$$\min_{\delta_p} J = \int_0^\infty \left(z^T Q z + u^T R u\right)\,\mathrm{d}t = \int_0^\infty \left(Q_{11}A_{z_m}^2 + R_{11}\delta_p^2\right)\,\mathrm{d}t \tag{3}$$

where

$$z = A_{z_m} = Hx + Lu = C_{11}\alpha + D_{11}\delta_p$$

Using the results of the previous subsections, this optimal control problem can be written as

$$\min_{\delta_p} J = \int_0^\infty \left(x^T Q x + 2x^T S u + u^T R u\right)\,\mathrm{d}t$$

where

$$Q = \begin{bmatrix} Q_{11}C_{11}^2 & 0 \\ 0 & 0 \end{bmatrix} \qquad S = \begin{bmatrix} Q_{11}C_{11}D_{11} \\ 0 \end{bmatrix} \qquad R = \left(Q_{11}D_{11}^2 + R_{11}\right)$$

As previously shown, the optimal solution is

$$u_{opt} = (I + K_{opt}C^{-1}D)^{-1}K_{opt}C^{-1}y \tag{4}$$

where $K_{opt} = -R^{-1}\left(B^T P + S^T\right)$ and P is the stabilizing solution to

$$(A - BR^{-1}S^T)^T P + P(A - BR^{-1}S^T) - PBR^{-1}B^T P + \left(Q - SR^{-1}S^T\right) = 0$$

D. Tracking Solution

Now let's turn our attention to the tracking problem. Here, we will define tracking as following a step command input, so that this is a set point regulator. The obvious optimization objective would be to use a weighted sum of the square of the error between the measured acceleration and the command, along with the control usage. In the tracking problem we will minimize the cost function

$$\begin{aligned} \min_{\delta_p} J &= \int_0^\infty \left[Q_{11} \left(A_{z_m} - K_{ss} A_{z_c} \right)^2 + R_{11} \delta_p^2 \right] \, \mathrm{d}t \\ \text{s.t.} \quad \dot{x} &= Ax + Bu \\ y &= Cx + Du - \tilde{K}_{ss} r \end{aligned}$$

$$\tilde{K}_{ss} = \begin{bmatrix} K_{ss} \\ 0 \end{bmatrix}$$

Note that a K_{ss} term is included on the command to ensure a zero steady-state error to a step. The general statement of the problem is

$$\min_u J = \int_0^\infty \left[\left(z - K_{ss} r \right)^T Q \left(z - K_{ss} r \right) + u^T R u \right] \, \mathrm{d}t$$

Let

$$\tilde{z} = z - z_{ss} = z - K_{ss} r$$

Given this, the problem is equivalent to the regulator problem

$$\begin{aligned} \min_u J &= \int_0^\infty \left(\tilde{z}^T Q \tilde{z} + u^T R u \right) \, \mathrm{d}t \\ \text{s.t.} \quad \dot{x} &= Ax + Bu \\ y &= Cx + Du - \tilde{K}_{ss} r \\ \tilde{z} &= Hx + Lu - K_{ss} r \end{aligned}$$

Let's turn to the determination of the steady state gain such that the command is followed. The optimal control can be written as

$$\begin{aligned} u &= K_{opt} \begin{bmatrix} A_{z_m} - K_{ss} A_{z_c} \\ q_m \end{bmatrix} \\ &= K_{opt} \begin{bmatrix} Hx + Lu - K_{ss} A_{z_c} \\ q_m \end{bmatrix} \\ &= K_{opt} \left[Cx + Du \right] - K_{opt} \begin{bmatrix} K_{ss} A_{z_c} \\ 0 \end{bmatrix} \end{aligned}$$

Thus the control is

$$u = \left[I - K_{opt} D \right]^{-1} K_{opt} \left[Cx - \begin{bmatrix} K_{ss} A_{z_c} \\ 0 \end{bmatrix} \right]$$

The closed loop system can be written as

$$\begin{aligned} \dot{x}_c &= A_c x_c + B_c A_{z_c} \\ A_z &= C_c x_c + D_c A_{z_c} \end{aligned}$$

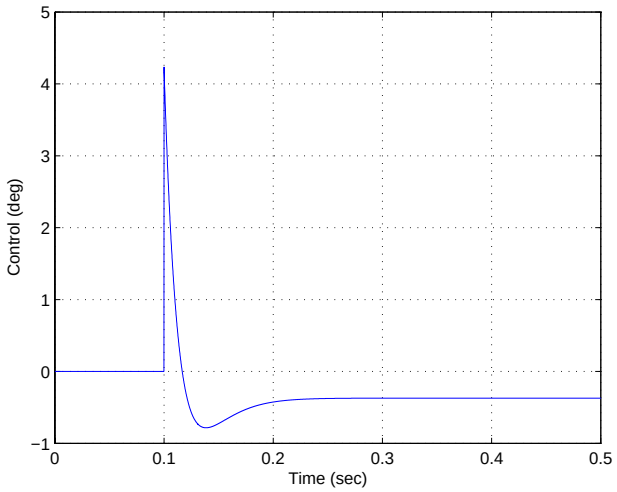

Figure 1. Optimal Control for the Tracking Problem

where

$$\begin{aligned} A_c &= A + B\left[I - K_{opt}D\right]^{-1} K_{opt}C \\ B_c &= -B\left[I - K_{opt}D\right]^{-1} K_{opt}\begin{bmatrix} K_{ss} \\ 0 \end{bmatrix} = -B_c' K_{ss} \\ C_c &= H + L\left[I - K_{opt}D\right]^{-1} K_{opt}C \\ D_c &= -L\left[I - K_{opt}D\right]^{-1} K_{opt}\begin{bmatrix} K_{ss} \\ 0 \end{bmatrix} = -D_c' K_{ss} \end{aligned}$$

and

$$\begin{aligned} B_c' &= B\left[I - K_{opt}D\right]^{-1} K_{opt}\begin{bmatrix} 1 \\ 0 \end{bmatrix} \\ D_c' &= L\left[I - K_{opt}D\right]^{-1} K_{opt}\begin{bmatrix} 1 \\ 0 \end{bmatrix} \end{aligned}$$

In order to insure zero steady state error

$$\begin{aligned} \lim_{s\to 0}\frac{A_z}{A_{z_c}} &= 1 \\ &= -C_c A_c^{-1} B_c + D_c \\ &= \left[C_c A_c^{-1} B_c' - D_c'\right] K_{ss} \end{aligned}$$

Therefore

$$K_{ss} = \left[C_c A_c^{-1} B_c' - D_c'\right]^{-1}$$

The unstable plant example with the initial conditions equal to zero and a command of $1g$ applied at $t = 0.1$ sec is used, with the weights chosen as $Q_{11} = 2.0$ and $R_{11} = 1.0$. The optimal gains are the same as for the regulator problem. The closed loop optimal solution is shown in Figures 1 and 2.

The closed loop optimal control law is

$$u_{opt} = \begin{bmatrix} -0.0395 & 0.1568 \end{bmatrix}\begin{bmatrix} A_{z_m} - K_{ss}A_{z_c} \\ q_m \end{bmatrix}$$

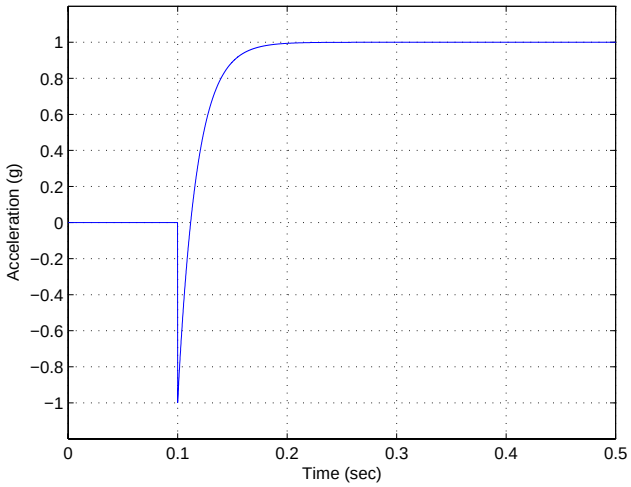

Figure 2. Optimal Step Response for the Tracking Problem

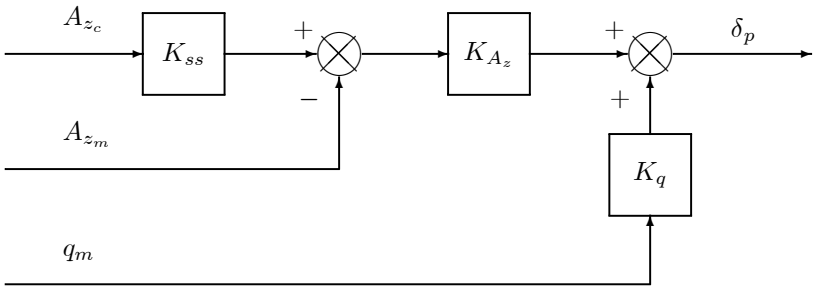

Figure 3. Two Loop Autopilot Topology

For this example, $K_{ss} = 0.8735$. The two loop topology is shown in Figure 3.

The sign convention needs to be addressed. The sign convention used is such that the feedback gains are usually positive. In all cases the controller is defined, including the sign of the feedback term, before the gains are presented. This is the convention used in all the topology figures throughout this paper. The solution to the optimal control problem assumes a positive feedback and the signs on the individual gains can be negative or positive. With that said, the gains for the example problem as shown in Figure 3 are

$$\begin{bmatrix} K_{ss} \\ K_{A_z} \\ K_q \end{bmatrix} = \begin{bmatrix} 0.8735 \\ 0.0395 \\ 0.1568 \end{bmatrix}$$

Clearly, no integrator is needed in the optimal solution and the regulation problem solves the tracker problem. It should be noted that there is a large, almost instantaneous non-minimum phase response. The large undershoot (the same magnitude as the command) is caused by having the system capable of infinite rate while moving the fin. Note: a canard controlled missile will not have the problem of moving in the wrong direction and the two state system minimizing the weighted integral of the acceleration error and control deflection may well be the way to pose the autopilot design problem. However, it seems likely the

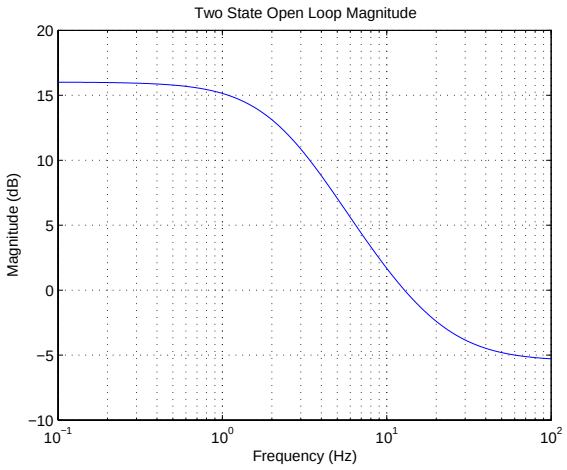

Figure 4. Two State Open Loop Magnitude

canard controlled missile will have a different problem in that Control Actuation System (CAS) dynamics will have to be included so that the command doesn't produce an instantaneous response at the commanded G level for high values of the acceleration error weighting. In other words, it is easy to make over-responsive solutions for canard controlled missiles that will be susceptible to noise and unmodeled dynamics. The weight on the acceleration error must be small enough so that there is a delay in achieving the desired G level. It is interesting to note that for non-minimum phase systems there is a limit as to how fast the system will respond with this cost function. The value of Q_{11} for this example is 2, but a value of 1000 gives about the same gains. It seems that once the initial response is equal to the command, the limit on the speed of response using this optimal control problem is defined. For minimum phase systems this is not the case.

Now let's look at the open loop Bode plot of the optimal system of the example. The loop will be broken at the input to the plant. This will give a measure of robustness. Writing the plant as a transfer function instead of in state space, the plant is

$$\frac{A_{z_m}}{\delta_p} = \frac{N_\delta^{A_z}}{\Delta}$$

and

$$\frac{q_m}{\delta_p} = \frac{N_\delta^{q}}{\Delta}$$

The open loop transfer function is

$$\frac{\delta_{out}}{\delta_{in}} = \frac{K_q N_\delta^q - K_{A_z} N_\delta^{A_z}}{\Delta}$$

For the example this transfer function is

$$\frac{\delta_{out}}{\delta_{in}} = \frac{0.5334s^2 - 52.6178s - 1835}{s^2 + 1.06s - 290.26}$$

The Bode Plots are shown in Figures 4 and 5. The optimal solution has a crossover frequency of about 12 Hz. Notice how the phase starts at -180 degrees because it is non-minimum phase.

IV. Penalizing the Control Rate – Three Loop Topologies

Since the previous setup required infinite control rate we could penalize the control rate instead of the control deflection. The cost function would then be

$$\min_{\dot{\delta}_p} J = \int_0^\infty \left(Q_{11} A_{z_m}^2 + R_{11} \dot{\delta}_p^2 \right) \, \mathrm{d}t$$

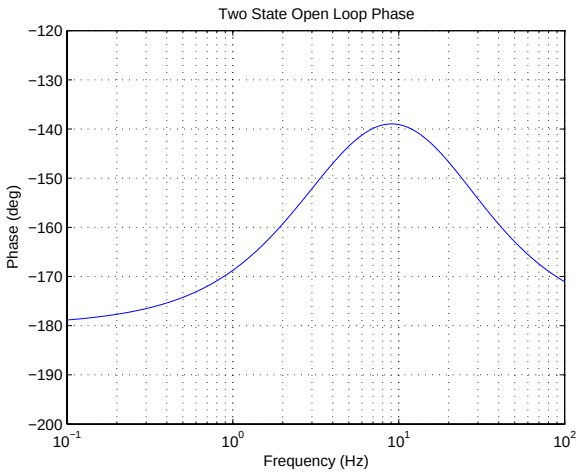

Figure 5. Two State Open Loop Phase

Therefore, we need the control rate as the input to the system. We can augment the dynamic system with the additional differential equation

$$\dot{\delta}_p = u$$

and add the control as a state. The regulator problem is then

$$\begin{aligned} \min_{\dot{\delta}_p} J &= \int_0^\infty \left(Q_{11} A_{z_m}^2 + R_{11} \dot{\delta}_p^2 \right) \mathrm{d}t \\ \text{s.t.} \quad \dot{x}_a &= A_a x_a + B_a u_a \\ y &= C_a x_a + D_a u_a \\ z &= H_a x_a + L_a u_a \end{aligned}$$

The actual determination of the gains was made using

$$Q_a = H_a^T Q_{11} H_a \qquad\qquad R_a = R$$

The actual MATLAB call is

$$[P, eigAcl, -K_{opt}] = care(A_a, B_a, Q_a, R_a)$$

We will also switch to a tracking problem at this point, since we know it has the same solution as the regulator problem. Thus, we wish to solve

$$\begin{aligned} \min_{\dot{\delta}_p} J &= \int_0^\infty \left[Q_{11} \left(A_{z_m} - K_{ss} A_{z_c} \right)^2 + R_{11} \dot{\delta}_p^2 \right] \mathrm{d}t \\ \text{s.t.} \quad \dot{x} &= Ax + Bu \\ y &= Cx + Du - \tilde{K}_{ss} r \end{aligned} \tag{5}$$

We need an additional measurement if we don't want to create an estimator, so let's assume the control deflection is indeed measurable. The system would then become

$$\begin{aligned} \dot{x}_1 &= A_1 x_1 + B_1 u_1 \\ y_1 &= C_1 x_1 + D_1 u_1 - \tilde{K}_{ss} r \\ z &= H_1 x_1 + L_1 u_1 - K_{ss} r \end{aligned}$$

where

$$x_1 = \begin{bmatrix} \alpha \\ q \\ \delta_p \end{bmatrix} \qquad u_1 = \dot{\delta}_p \qquad y_1 = \begin{bmatrix} A_{z_m} - K_{ss} r \\ q_m \\ \delta_p \end{bmatrix}$$

and

$$\begin{aligned} A_1 &= \begin{bmatrix} A & B \\ [0] & 0 \end{bmatrix} \qquad B_1 = \begin{bmatrix} [0] \\ 1 \end{bmatrix} \qquad \tilde{K}_{ss} = \begin{bmatrix} K_{ss} \\ [0] \end{bmatrix} \\ C_1 &= \begin{bmatrix} C & D \\ [0] & 1 \end{bmatrix} \qquad D_1 = \begin{bmatrix} [0] \\ 0 \end{bmatrix} \qquad H_1 = C_1(1,:) \qquad L_1 = [0] \end{aligned}$$

A note on the notation; [0] denotes a zero matrix of the proper dimensions and $x()$ is the notation used by MATLAB to designate portions of a larger matrix. For example $C_1(1,:)$ is the first row of the C_1 matrix. Since the plant is strictly proper the optimal solution can be found using the coordinate transform

$$x_2 = C_1 x_1 = y_1$$

so that the dynamic system is

$$\begin{aligned} C_1^{-1}\dot{x}_2 &= A_1 C_1^{-1} x_2 + B_1 u \\ y &= x_2 \end{aligned}$$

or

$$\begin{aligned} \dot{x}_2 &= C_1 A_1 C_1^{-1} x_2 + C_1 B_1 u \\ y &= x_2 \end{aligned}$$

The optimal gains can be found using

$$[P, eigAcl, -K_{opt}] = care(C_1 A_1 C_1^{-1}, C_1 B_1, Q_2, R_2)$$

where

$$Q_2 = \left(C_1^{-1}\right)^T H_1^T Q_{11} H_1 C_1^{-1} \qquad R_2 = R_{11}$$

The optimal tracking solution is

$$u_{opt} = \begin{bmatrix} -2.0740 & 11.7514 & -119.0269 \end{bmatrix} \begin{bmatrix} A_{z_m} - K_{ss} A_{z_c} \\ q_m \\ \delta_p \end{bmatrix}$$

Following the previous derivation the steady state gain can be determined from the same equations that have been transformed into the new variables with $D_1 = L_1 = 0$. Let

$$\begin{aligned} A_c &= C_1 \left(A_1 C_1^{-1} + B_1 K_{opt}\right) \\ B_c &= -C_1 B_1 K_{opt} \begin{bmatrix} K_{ss} \\ 0 \\ 0 \end{bmatrix} = -B_c' K_{ss} \\ C_c &= H_1 C_1^{-1} \end{aligned}$$

and

$$B_c' = C_1 B_1 K_{opt} \begin{bmatrix} 1 \\ 0 \\ 0 \end{bmatrix}$$

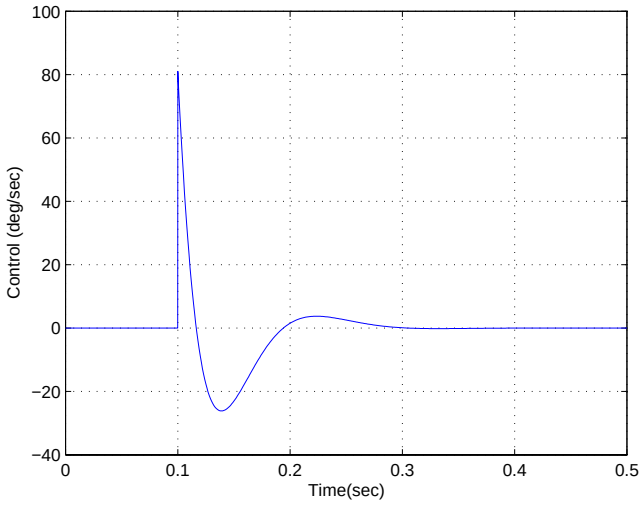

Figure 6. Control Rate Usage

In order to insure zero steady state error

$$\begin{aligned}\lim_{s\to 0}\frac{A_z}{A_{z_c}} &= 1\\ &= -C_c A_c^{-1} B_c\\ &= \left[C_c A_c^{-1} B_c'\right] K_{ss}\end{aligned}$$

Therefore

$$K_{ss} = \left[C_c A_c^{-1} B_c'\right]^{-1}$$

For this example $K_{ss} = 0.6819$. The results of the feedback simulation are presented in Figures 6 and 7.

For this set up, the plant is now strictly proper and there are three states. Since the control rate is penalized the non-minimum phase behavior is not as pronounced as in the original set up. This is because direct feed through of the acceleration command to the actuator is not allowed. Since

$$\dot{\delta}_p = u_{opt}$$

we can solve for the control deflection by substitution. The optimal control results in a first order dynamic equation in δ_p. The fin command could be written as

$$\delta_p = \frac{119.0269}{s+119.0269}\begin{bmatrix} -0.0174 & 0.0987 \end{bmatrix}\begin{bmatrix} A_{z_m} - K_{ss}A_{z_c} \\ q_m \end{bmatrix}$$

As can be seen the gains are less for this solution than the two state problem. Actually the gains and the response approach the solution to the first problem as the weight on the acceleration state is made large, but the solution cannot reach the previous solution time response because of the restriction on the direct feed through of the command which results in a pure lag that gets faster and faster but never goes away.

At this point, two different optimal control problems have been identified as potential problem statements for autopilot design. The difference is not in how the state weight enters the cost function but instead the variable used for the control weighting. The first formulation uses the fin deflection, the second uses the fin rate. The first formulation leads to a direct feed through of the acceleration command into the plant and since there is a "D" term in the plant, the acceleration response, for a tail controlled missile, instantly jumps in the wrong direction at the start of the step response. These are two loop topologies, as they have two feedback gains. The second approach does not allow the direct feed through of the command into the plant. This is accomplished by augmenting an integrator to the system. This approach results in a slower response

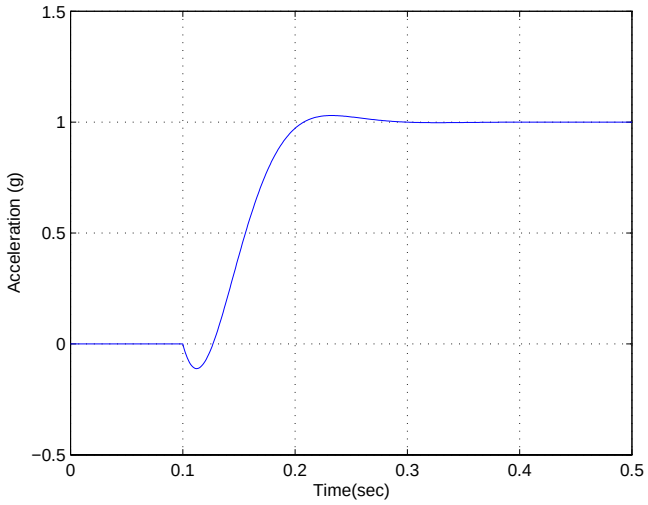

Figure 7. Acceleration Response to a Step Input

than the first, and is called a three loop topology, as it has three feedback gains. In general, it is much more practical for missile autopilot design, and therefore we will examine it more closely. In the follow-on paper by Mracek and Ridgely,[3] we will look at all possible three loop topologies, given the performance index defined thus far.

A. LQR Transformation of the Three Loop Topology

Now let's try to solve the problem slightly differently. In the example of Section 4, we made the three loop controller look more like a two loop controller by assuming the control deflection was not available, and using a filter instead. Note that this is still a three loop topology, however, as the command is filtered. Let's try to find a coordinate transformation so that we don't need the filter in the problem formulation. Following Adams and Conrardy,[2] the dynamic system is

$$\begin{aligned} \dot{x} &= Ax + Bu \\ y &= Cx + Du - \tilde{K}_{ss} r \end{aligned}$$

where

$$x = \begin{bmatrix} \alpha \\ q \end{bmatrix} \qquad u = \delta_p \qquad y = \begin{bmatrix} A_{z_m} - K_{ss} A_{z_c} \\ q_m \end{bmatrix}$$

and

$$\tilde{K}_{ss} = \begin{bmatrix} K_{ss} \\ 0 \end{bmatrix}$$

The states are augmented with the control, the control is replaced with the derivative of the control and the output is augmented with the derivative of the angular rate. Notice that no new information is introduced into the plant. The additional dynamic equation is the identity $\dot{\delta p} = u_1 = \dot{\delta p}$. The only impact is that a pole is introduced at the origin. The plant is rewritten as

$$\begin{aligned} \dot{x}_1 &= A_1 x_1 + B_1 u_1 \\ y_1 &= C_1 x_1 + D_1 u_1 - \tilde{K}_{ss1} r \\ \tilde{z}_1 &= H_1 x_1 + L_1 u_1 - K_{ss} r \end{aligned} \tag{6}$$

where

$$x_1 = \begin{bmatrix} \alpha \\ q \\ \delta_p \end{bmatrix} \qquad u_1 = \dot{\delta}_p \qquad y_1 = \begin{bmatrix} A_{z_m} - K_{ss} A_{z_c} \\ q_m \\ \dot{q}_m \end{bmatrix} \qquad \tilde{K}_{ss1} = \begin{bmatrix} K_{ss} \\ 0 \\ 0 \end{bmatrix}$$

Using the aforementioned notation, the transformation is

$$A_1 = \begin{bmatrix} A & B \\ [0] & 0 \end{bmatrix} \qquad B_1 = \begin{bmatrix} [0] \\ 1 \end{bmatrix}$$

$$C_1 = \begin{bmatrix} C & D \\ A(2,:) & B(2,:) \end{bmatrix} \qquad D_1 = \begin{bmatrix} [0] \\ 0 \end{bmatrix}$$

The state transformation $x_1 = C_1^{-1} y_1$ can now be used. The transformed plant is

$$\begin{aligned} \dot{x}_2 &= A_2 x_2 + B_2 u_2 \\ y_2 &= x_2 \end{aligned}$$

where

$$x_2 = \begin{bmatrix} A_{z_m} \\ q_m \\ \dot{q}_m \end{bmatrix} \qquad u_2 = \dot{\delta}_p$$

and

$$A_2 = C_1 A_1 C_1^{-1} \qquad B_2 = C_1 B_1$$

Now we can set up the cost function

$$\min_{\dot{\delta}_p} J = \int_0^\infty \left[Q_{11} \left(A_{z_m} - K_{ss} A_{z_c} \right)^2 + R_{11} \dot{\delta}_p^2 \right] \mathrm{d}t$$

so that

$$H_1 = C_1(1,:) \qquad L_1 = [0]$$

The LQR solution can now be determined in a straightforward manner. The gains are found through

$$[P, eigAcl, -K_{opt}] = care(A_2, B_2, Q_2, R_2)$$

where

$$Q_2 = \left(C_1^{-1} \right)^T H_1^T Q_{11} H_1 C_1^{-1} \qquad R_2 = R_{11}$$

The control law is

$$u_{opt} = K_{opt} \begin{bmatrix} A_{z_m} - K_{ss} A_{z_c} \\ q_m \\ \dot{q}_m \end{bmatrix} = \dot{\delta}_p \tag{7}$$

where K_{ss} is determined from

$$K_{ss} = \left[C_c A_c^{-1} B_c' \right]^{-1}$$

where

$$\begin{aligned} A_c &= A_2 + B_2 K_{opt} \\ B_c &= -B_2 K_{opt} \begin{bmatrix} K_{ss} \\ 0 \\ 0 \end{bmatrix} = -B_c' K_{ss} \quad \text{where } B_c' = B_2 K_{opt} \begin{bmatrix} 1 \\ 0 \\ 0 \end{bmatrix} \\ C_c &= H_1 C_1^{-1} \end{aligned}$$

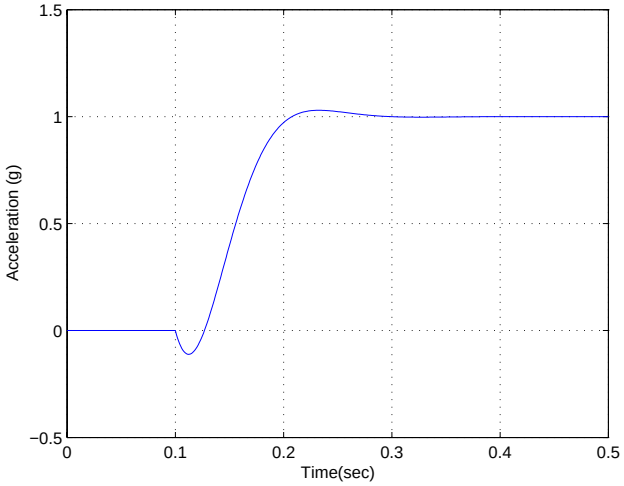

Figure 8. Closed Loop Step Response

Using these equations with the unstable plant and the values used for Q_{11} and R_{11} thus far results in

$$K_{opt} = \begin{bmatrix} -1.3028 & 11.7514 & 0.3277 \end{bmatrix} \qquad K_{ss} = 1.0855$$

Notice how this approach has as the cost function a weighting on the acceleration error and the control rate, just as in the example in Section 4 above.

In the current setup, $\dot{q}_m$ is not measurable. Notice that the optimal control u_2 is actually $\dot{\delta}_p$, so if we simply integrate both sides of Equation 7 since we have a linear system, the control δ_p would be (assuming constant gains at the design point)

$$\delta_p = K_{opt} \begin{bmatrix} \int (A_{z_m} - K_{ss} A_{z_c}) \ \mathrm{d}t \\ \int q_m \ \mathrm{d}t \\ \int \dot{q}_m \ \mathrm{d}t \end{bmatrix} = K_{opt} \begin{bmatrix} \int (A_{z_m} - K_{ss} A_{z_c}) \ \mathrm{d}t \\ \int q_m \ \mathrm{d}t \\ q_m \end{bmatrix}$$

This formulation results in the so called classic three loop autopilot. The closed loop step response using this formulation is presented in Figure 8, which is identical to Figure 7.

The classical three loop topology is presented in Figure 9. The optimal controller is given by

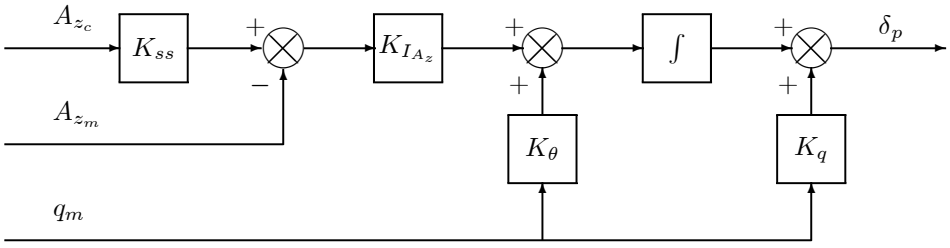

Figure 9. Classic Three Loop Topology

$$K_{I_{A_Z}} = 1.3028 \qquad K_\theta = 11.7514 \qquad K_q = 0.3277 \qquad K_{ss} = 1.0855$$

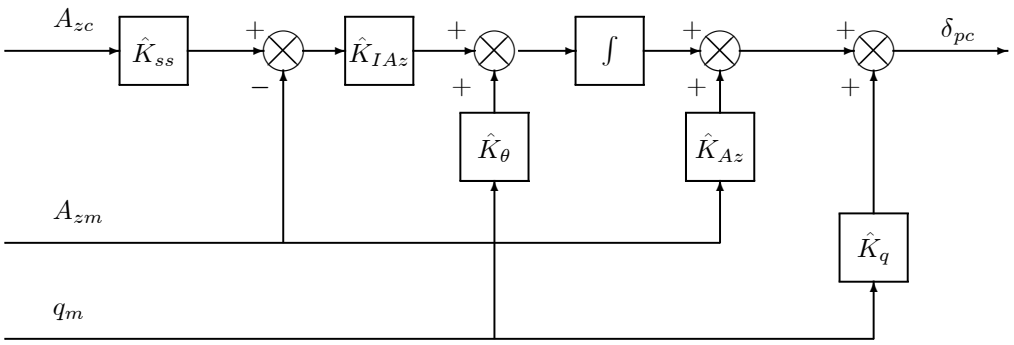

Figure 10. Four Loop Autopilot Topology

Clearly, since we know our plant, we could reconstruct the angular acceleration in terms of A_{z_m}, q_m, and δ_p and we would find that the optimal control would be exactly the same as we found previously. We will see this is a general result (same closed loop system), but there are definite differences between the two nonetheless.

The question then is which of the topologies are "better"? The closed loop responses are identical. However, the feedback mechanisms are different and therefore the open loop properties will be different. This means that different topologies will have different robustness properties for a given level of performance. This is examined in a follow-on paper.[3]

V. Neoclassic Four Loop Topology

The neoclassic four loop topology is shown in Figure 10. From this figure we see that the control law is given by

$$\delta_{pc} = \int \left[\hat{K}_{I_{A_z}}(\hat{K}_{ss}A_{z_c} - A_{z_m}) + \hat{K}_{\theta}q_m\right] \mathrm{d}t + \hat{K}_{A_z}A_{z_m} + \hat{K}_q q_m$$

or with constant gains

$$\delta_{pc} = \hat{K}_{I_{A_z}}\hat{K}_{ss}\int A_{z_c}\,\mathrm{d}t - \hat{K}_{I_{A_z}}\int A_{z_m}\,\mathrm{d}t + \hat{K}_{A_z}A_{z_m} + \hat{K}_{\theta}\int q_m\,\mathrm{d}t + \hat{K}_q q_m$$

The feedback portion of the neoclassic four loop autopilot is proportional plus integral on the angular rate and proportional plus integral on the linear acceleration. Again the acceleration command enters the system through an integrator. Clearly, setting $\hat{K}_{I_{A_z}} = K_{I_{A_z}}$, $\hat{K}_{\theta} = K_{\theta}$, $\hat{K}_q = K_q$, $\hat{K}_{ss} = K_{ss}$ and $\hat{K}_{A_z} = 0$, results in the neoclassic design reducing to the classic three loop design. The addition of the $\hat{K}_{A_z}$ gain gives added design flexibility without compromising the original design philosophy.

Now let's take a close look at the neoclassic four loop autopilot. Introduce a first order lag into the system that captures relevant unmodeled dynamics (we will tend to refer to these as CAS dynamics, but they can be general unmodeled dynamics reflected to the input of the plant). In other words, let

$$\dot{\delta}_p = \tau\left(\delta_{pc} - \delta_p\right)$$

Now let the states be augmented with the fin position and fin command, and the control be set to the derivative of the fin command. The output is the derivative of the linear acceleration, the derivative of the angular rate, the linear acceleration and the angular rate. The new state space representation is

$$\begin{aligned} \dot{x}_1 &= A_1x_1 + B_1u_1 \\ y_1 &= C_1x_1 + D_1u_1 - \tilde{K}_{ss2}r \end{aligned} \tag{8}$$

where

$$x_1 = \begin{bmatrix} \alpha \\ q \\ \delta_p \\ \delta_{pc} \end{bmatrix} \qquad u_1 = \dot{\delta}_{pc} \qquad y_1 = \begin{bmatrix} A_{z_m} - K_{ss} r \\ q_m \\ \dot{A}_{z_m} \\ \dot{q}_m \end{bmatrix} \qquad \hat{K}_{ss2} = \begin{bmatrix} K_{ss} \\ 0 \\ 0 \\ 0 \end{bmatrix}$$

The new plant is

$$A_1 = \begin{bmatrix} A & B & [0] \\ [0] & -\tau & \tau \\ [0] & 0 & 0 \end{bmatrix} \qquad B_1 = \begin{bmatrix} [0] \\ 0 \\ 1 \end{bmatrix}$$

The output can be determined from

$$\begin{bmatrix} \dot{A}_{z_m} \\ \dot{q}_m \end{bmatrix} = C\dot{x} + D\dot{\delta}_p$$

where

$$\dot{\delta}_p = \tau \left(\delta_{pc} - \delta_p \right)$$

The output equations are then

$$C_1 = \begin{bmatrix} C & D & [0] \\ CA & CB - D\tau & D\tau \end{bmatrix} \qquad D_1 = \begin{bmatrix} [0] \\ [0] \end{bmatrix}$$

Again the system is strictly proper, but this time additional dynamics are included in the plant model. Following the development of Section IV.A, we will minimize the performance index

$$\min_{\dot{\delta}_{p_c}} J = \int_0^\infty \left[Q_{11} \left(A_{z_m} - K_{ss} A_{z_c} \right)^2 + R_{11} \dot{\delta}_{pc}^2 \right] \, \mathrm{d}t$$

The optimal LQR problem can be solved directly, and the control is

$$\delta_{pc} = K \begin{bmatrix} -\int \left(A_{z_m} - K_{ss} A_{z_c} \right) \, \mathrm{d}t \\ \int q_m \, \mathrm{d}t \\ A_{z_m} \\ q_m \end{bmatrix}$$

where

$$K = \begin{bmatrix} K_{I_{A_z}} \\ K_\theta \\ K_{A_z} \\ K_q \end{bmatrix} = \begin{bmatrix} 1.2241 \\ 20.0583 \\ 0.0524 \\ 0.4182 \end{bmatrix}$$

and $K_{ss} = 1.1553$ for $\tau = 20Hz$, $Q_{11} = 2$ and $R_{11} = 1$. This topology can now be examined. First, the frequency of the additional first order dynamics is varied and the optimal gains are computed. It is shown in Figure 11 that all four gains go to the classic three loop topology gain values as the frequency becomes large.

Next, closed-loop step responses for four different CAS frequencies were examined, as seen in Figure 12. These are plotted against the responses of the 3-loop optimal gains with the CAS dynamics present in the system (indicating robustness of the 3-loop design to the CAS dynamics). Note that, as expected, the 4-loop designs are very robust to the CAS dynamics, as they are designed with explicit knowledge of the dynamics. The 3-loop designs start to suffer badly as the CAS dynamics approach the bandwidth of the system.

Finally, we will examine the robustness of the 4-loop controller versus the 3-loop controller at the input and output of the plant and to plant variations when various CAS dynamics are present in the system. Figure 13 shows the vector margin (margin defined from nearness to the critical point on the Nyquist plot

$$\sigma_0 = \min_\omega \left| 1 + L(j\omega) \right|$$

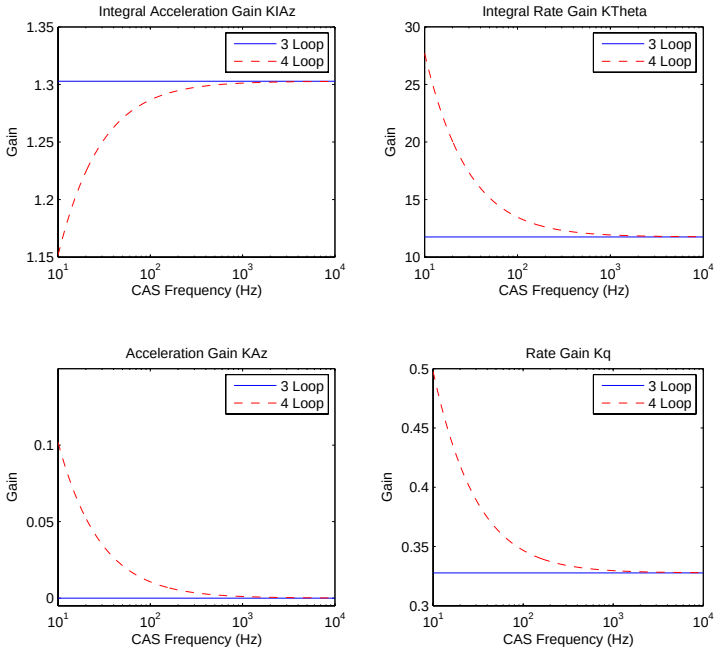

Figure 11. Gain Variation in the 4 Loop Topology with CAS Frequency

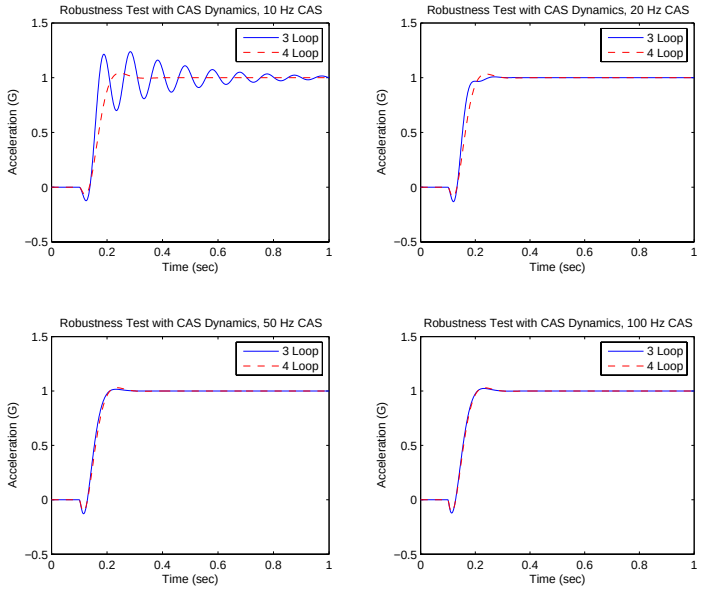

Figure 12. Step Responses for the 3 and 4 Loop Controllers with CAS Dynamics Present

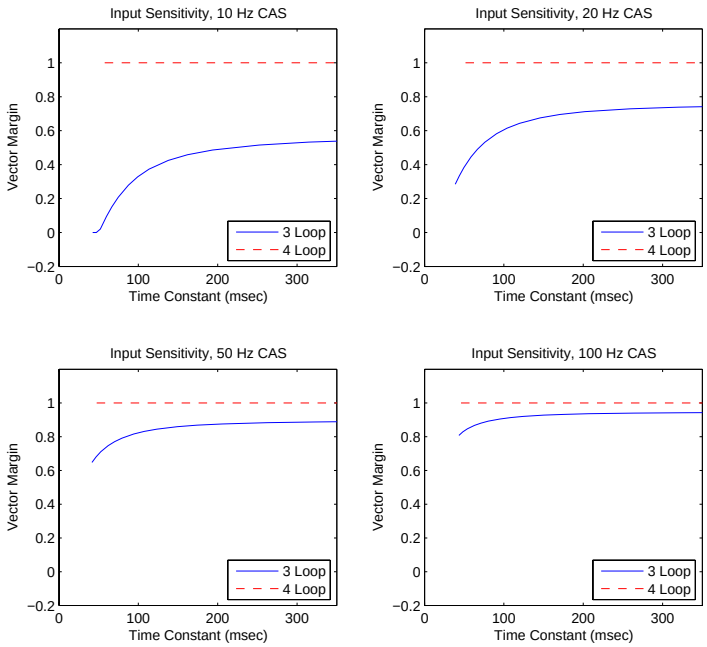

Figure 13. Vector Margin at the Plant Input for the 3- vs. 4-Loop Topology with Various CAS Dynamics

where $L(j\omega)$ is the loop transfer function) broken at the input to the plant plotted against rise time (various choices of Q_{11}) for various CAS frequencies. Note that the CAS dynamics "eat up" some of the ideal margin of 1.0 in the 4-loop topology, and this is worse as the CAS frequency becomes lower. Plant uncertainties are examined in Figure 14. Again, the CAS dynamics tend to "eat up" much of the robustness to plant variations in the 3-loop system, and this effect is worse as the CAS frequency gets lower. For the actual method of determining the robustness to plant variations see Mracek and Ridgely.[3]

The results with the loops broken at the rate sensor and the accelerometer are shown in Figures 15 and 16, respectively. These show some very interesting results. In general, for slower systems (larger rise times) the 3-loop topology is "more robust" to output uncertainties than the 4-loop system. This is because the 4-loop topology is optimized for what looks like an input uncertainty, and must therefore give up something at the output. In general, the uncertainties at the output of the system are at higher frequencies than those at the input, so the uncertainty at the output will tend to be smaller over frequencies of interest. The designer would have to adjust this trade as appropriate for the particular system in question. In particular, this definitely implies that the margins at the output of the plant should be examined. Overall, the 4-loop topology looks very promising and further studies on this topology are warranted.

VI. Higher Order Dynamics

What if we include higher order dynamics in our model? Let's assume the unmodeled dynamics are such that

$$\ddot{\delta}_p = -(\tau_1 + \tau_2)\dot{\delta}_p + \tau_1\tau_2\left(\delta_{pc} - \delta_p\right)$$

Then let the plant states be augmented with the fin position, the fin rate and fin command and let the control be set to the derivative of the fin command. The outputs are the linear acceleration and the angular rate, the first derivative of the angular rate and the linear acceleration, the second derivative of the angular rate and the linear acceleration, and the fin command. We will not use all of these outputs, as seen shortly.

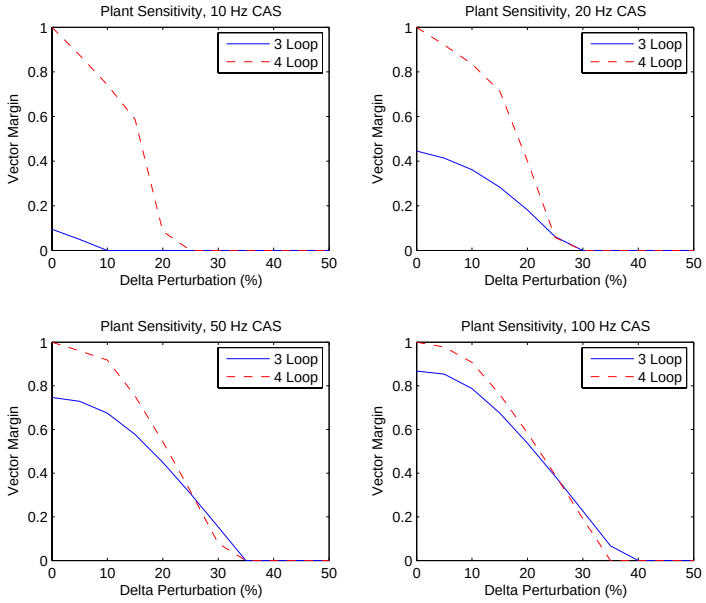

Figure 14. Vector Margin at the Plant Input with Different Plant Uncertainties 3- vs. 4-Loop Topology with Various CAS Dynamics

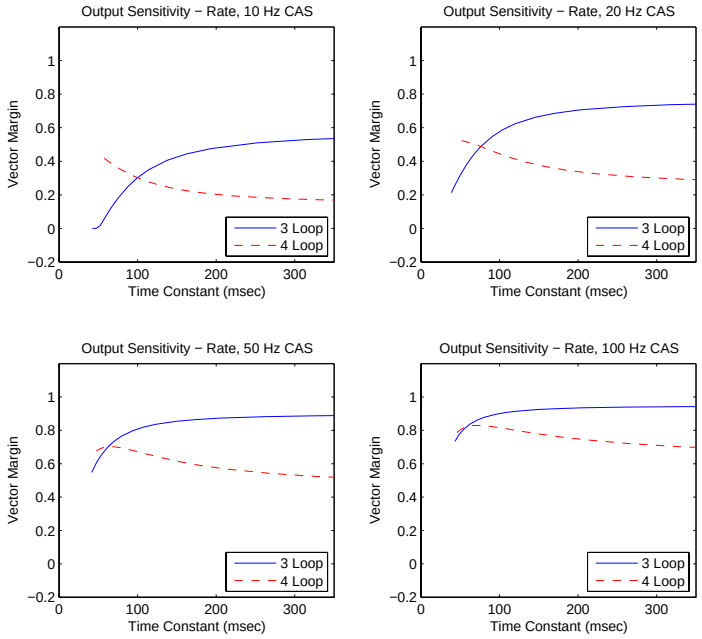

Figure 15. Vector Margin at the Rate Output for the 3- vs. 4-Loop Topology with Various CAS Dynamics

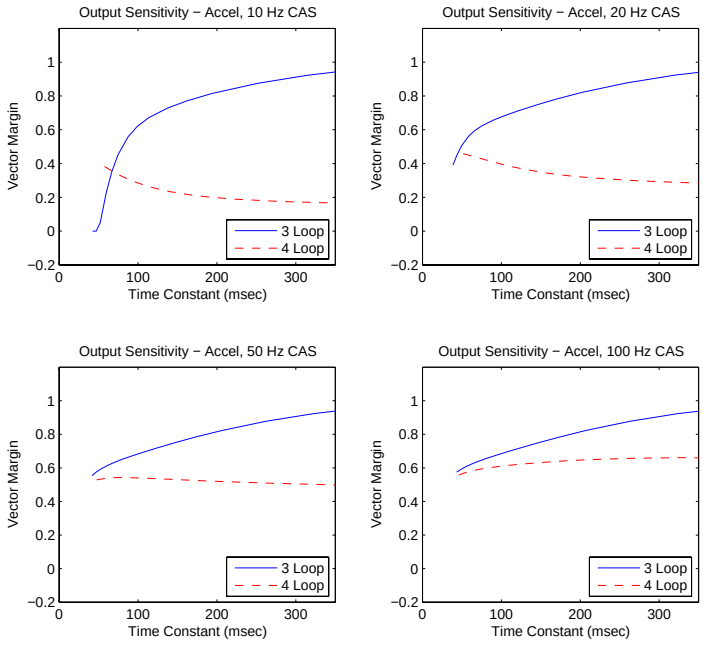

Figure 16. Vector Margin at the Accelerometer Output for the 3- vs. 4-Loop Topology with Various CAS Dynamics

The new state space representation is

$$\begin{aligned} \dot{x}_1 &= A_1 x_1 + B_1 u_1 \\ \bar{y} &= \bar{C} x_1 + \bar{D} u_1 - \tilde{K}_{ss3} r \end{aligned}$$

where

$$x_1 = \begin{bmatrix} \alpha \\ q \\ \delta_p \\ \dot{\delta}_p \\ \delta_{pc} \end{bmatrix} \qquad u_1 = \dot{\delta}_{pc} \qquad \bar{y} = \begin{bmatrix} A_{z_m} - K_{ss} r \\ q_m \\ \dot{A}_{z_m} \\ \dot{q}_m \\ \ddot{A}_{z_m} \\ \ddot{q}_m \\ \delta_{pc} \end{bmatrix} \qquad \tilde{K}_{ss3} = \begin{bmatrix} K_{ss} \\ 0 \\ 0 \\ 0 \\ 0 \\ 0 \\ 0 \end{bmatrix}$$

The state space matrices are then

$$A_1 = \begin{bmatrix} A & B & [0] & [0] \\ [0] & 0 & 1 & 0 \\ [0] & -\tau_1\tau_2 & -(\tau_1+\tau_2) & \tau_1\tau_2 \\ [0] & 0 & 0 & 0 \end{bmatrix} \qquad B_1 = \begin{bmatrix} [0] \\ 0 \\ 0 \\ 1 \end{bmatrix}$$

$$\bar{C} = \begin{bmatrix} C & D & [0] & [0] \\ CA & CB & D & [0] \\ --- & ------ & ------ & --- \\ CA^2 & CAB - \tau_1\tau_2 D & CB - (\tau_1+\tau_2)D & \tau_1\tau_2 D \\ [0] & 0 & 0 & 1 \end{bmatrix} \qquad \bar{D} = \begin{bmatrix} [0] \\ [0] \\ -- \\ [0] \\ 0 \end{bmatrix}$$

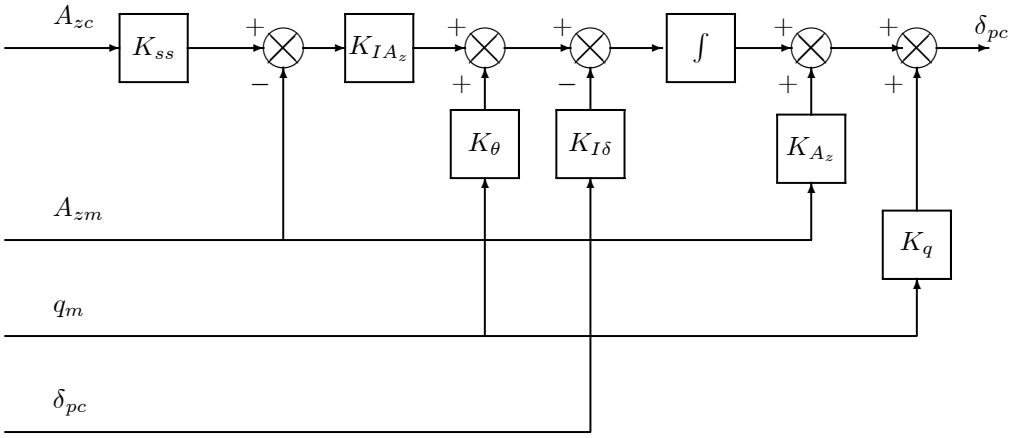

Figure 17. Five Loop Autopilot Topology

We only want 5 outputs, since we only have 5 states and we want C_1 to be invertible. Above the dashed lines in $\bar{C}$ and $\bar{D}$ represents 4 outputs we must keep, so that we need to choose 1 from the 3 below. We cannot choose $\ddot{q}_m$, since its D term is zero and that will leave C_1 with a column of zeros. If we choose $\ddot{A}_{z_m}$, then when we integrate $\dot{\delta}_{pc}$ to get the control law, we will still have an $\dot{A}_{z_m}$ term, which implies we would have PID control on the acceleration. While the derivative could be formed through the dynamics, this introduces additional noise and errors, so we will not pursue this further here. That only leaves δ_{pc} as a possible output (the last row), which results in

$$C_1 = \begin{bmatrix} C & D & [0] & [0] \\ CA & CB & D & [0] \\ [0] & 0 & 0 & 1 \end{bmatrix} \qquad D_1 = \begin{bmatrix} [0] \\ [0] \\ 0 \end{bmatrix}$$

The system is strictly proper and C_1^{-1} exists, but notice that we are back to the situation where not all of the outputs are directly measurable. While we can replace this with a lag, this leads to systems that are not as robust. In particular we should not expect the input vector margin to be unity. Again following the development of Section IV.A, we will minimize the performance index

$$\min_{\delta_{pc}} J = \int_0^\infty \left[Q_{11} \left(A_{z_m} - K_{ss} A_{z_c} \right)^2 + R_{11} \dot{\delta}_{p_c}^2 \right] \mathrm{d}t$$

The optimal LQR problem can be solved directly, and the control is

$$\delta_{pc} = K \begin{bmatrix} -\int \left(A_{z_m} - K_{ss} A_{z_c} \right) \mathrm{d}t \\ \int q_m \, \mathrm{d}t \\ A_{z_m} \\ q_m \\ -\int \delta_{pc} \, \mathrm{d}t \end{bmatrix}$$

where

$$K = \begin{bmatrix} K_{I_{A_z}} \\ K_\theta \\ K_{A_z} \\ K_q \\ K_{I_\delta} \end{bmatrix} = \begin{bmatrix} 1.8136 \\ 17.8562 \\ 0.0180 \\ 0.2772 \\ 87.7615 \end{bmatrix}$$

and $K_{ss} = 0.7798$ for $\tau_1 = \tau_2 = 20Hz$, $Q_{11} = 2$ and $R_{11} = 1$. The resulting 5-loop topology is shown in Figure 17.

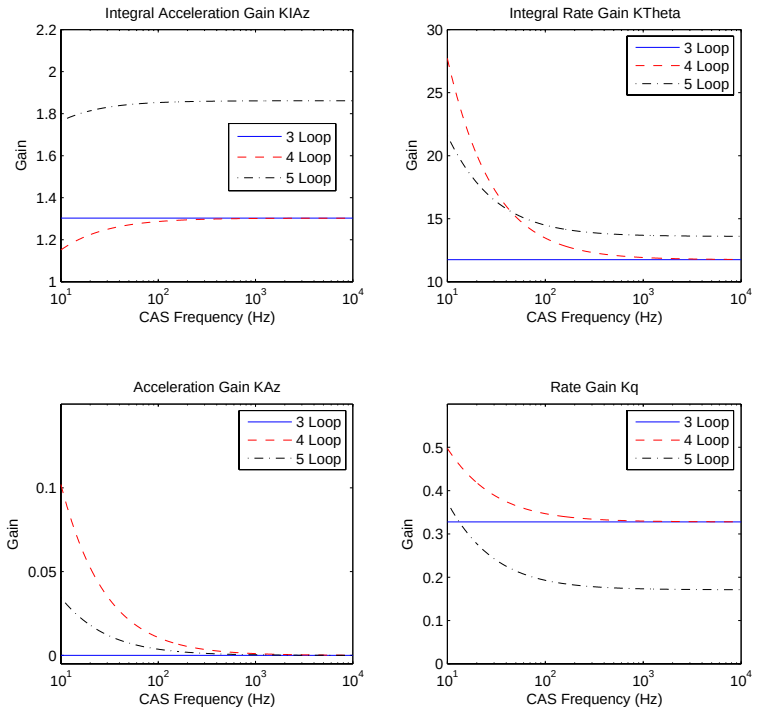

Figure 18. Gains for the 3-, 4-, and 5-Loop Systems

The gains for the classic 3-loop, the neoclassic 4-loop, and the 5-loop system above are given in Figures 18 and 19. Clearly, these gains do NOT go to the classic gains as the frequency of the additional dynamics gets large.

The time responses and various vector margins in the face of the CAS dynamics are shown in Figures 20 through 23. Note that all of these figures show the results for the 3- and 4-loop systems with the quadratic CAS dynamics included. The overall conclusion here is that the 4-loop topology is probably the superior one unless the frequency of the CAS dynamics is very low and a very fast response is required. Notice also the 5-loop did not recover the unity vector margin when the loop is broken at the input. In fact it has relatively poor performance for slower overall system response.

We will need to reformulate the feedback if we wish to recover the 4-loop and 3-loop characteristics. In particular, we will need to use the second derivative of the fin deflection as feedback, and to model the higher order dynamics as two cascaded real poles. The problem would be formulated as

$$\ddot{\delta}_p = -(\tau_1 + \tau_2)\dot{\delta}_p + \tau_1\tau_2\left(\delta_{p_c} - \delta_p\right)$$

$$A_1 = \begin{bmatrix} A & B & [0] & [0] \\ [0] & 0 & 1 & 0 \\ [0] & -\tau_1\tau_2 & -(\tau_1+\tau_2) & \tau_1\tau_2 \\ [0] & 0 & 0 & 0 \end{bmatrix} \qquad B_1 = \begin{bmatrix} [0] \\ 0 \\ 0 \\ 1 \end{bmatrix}$$

$$C = \begin{bmatrix} C & D & [0] & [0] \\ CA & CB & D & [0] \\ [0] & -\tau_1\tau_2 & -(\tau_1+\tau_2) & \tau_1\tau_2 \end{bmatrix} \qquad D = \begin{bmatrix} [0] \\ [0] \\ 0 \end{bmatrix}$$

Selecting the first time constant to $\tau_1 = 20(Hz)$ and letting the other time constant vary, the gains for four and five loop controllers are presented in Figures 24 and 25. The feedback would involve the rate of the

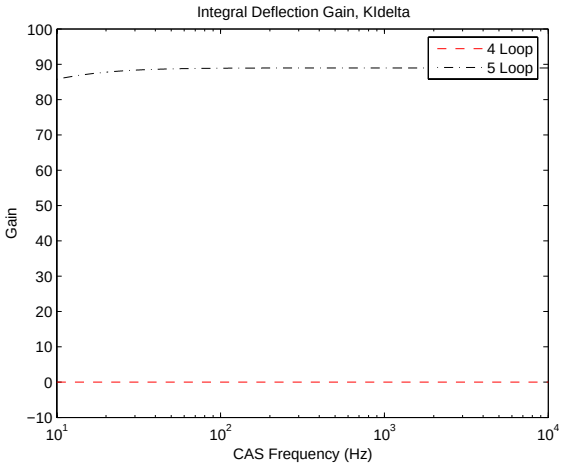

Figure 19. K_{I_δ} Gains for the 3-, 4-, and 5-Loop Systems

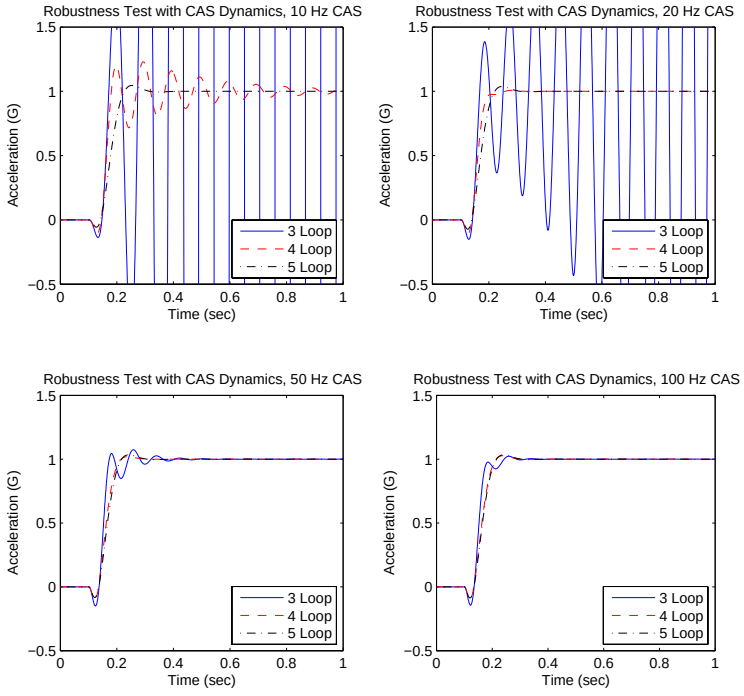

Figure 20. Time Responses for 3-, 4-, and 5-Loop Systems with CAS Dynamics Present

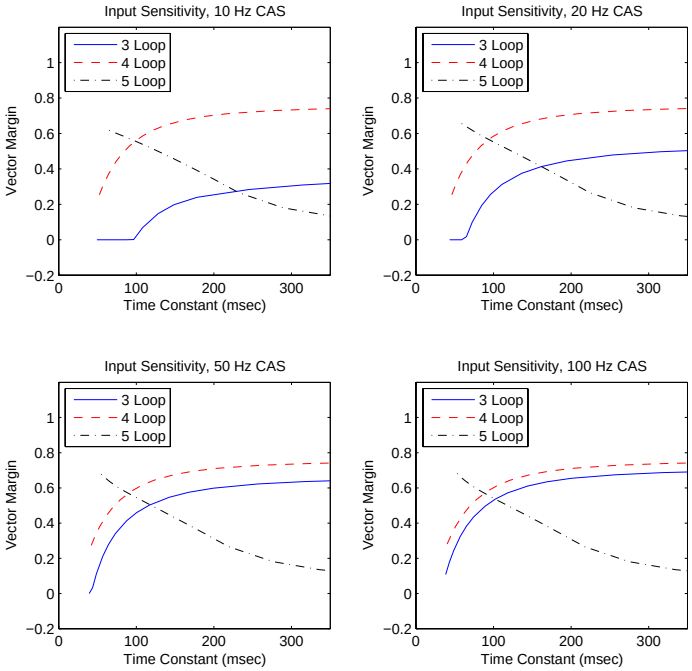

Figure 21. Vector Margins at the Plant Input for the 3-, 4-, and 5-Loop Systems with Varying CAS Frequencies

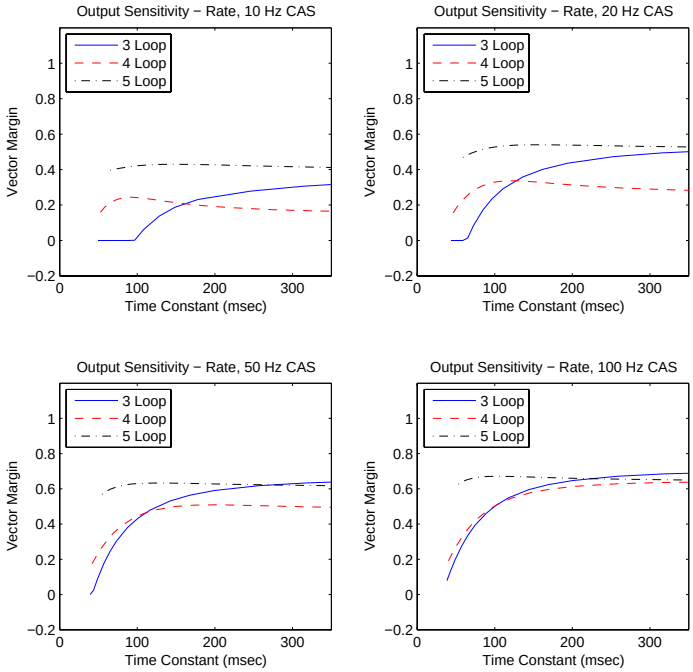

Figure 22. Vector Margins at the Rate Output for the 3-, 4-, and 5-Loop Systems with Varying CAS Frequencies

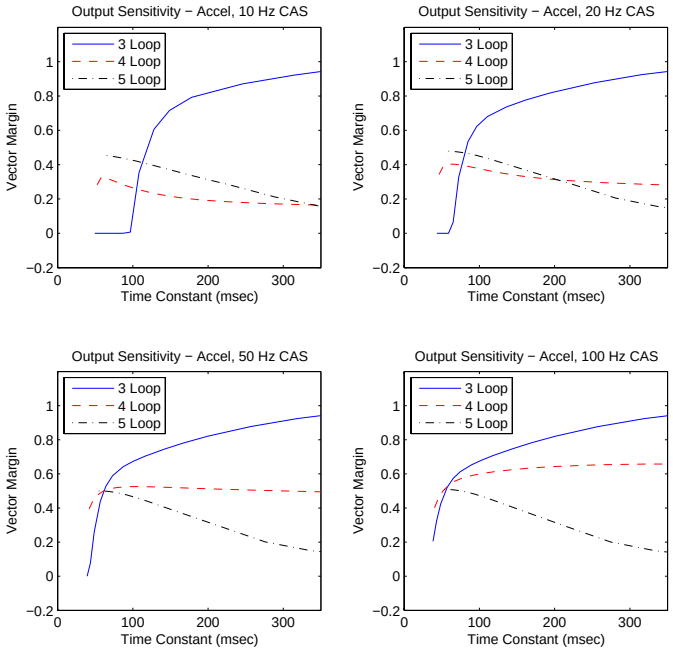

Figure 23. Vector Margins at the Acceleration Output for the 3-, 4-, and 5-Loop Systems with Varying CAS Frequencies

controller but this could easily be formed by using the transfer function and creating a lead.

$$\frac{\dot{\delta}_p}{\delta_{pc}} = \frac{\tau_1 \tau_2 s}{s^2 + (\tau_1 + \tau_2)s + \tau_1 \tau_2}$$

This implementation results in the robustness characteristics presented in Figures 26 to 28. Now the trends follow the same course as moving from the three to the four loop. The input sensitivity is now better for the five loop when compared to both the three and four loop systems. The input sensitivity is not unity because the loop is broken after the lead but before the CAS. The margins with the plant broken at the outputs continue to deteriorate as the system response is slower. It is interesting to note the margins do not change significantly for the four CAS frequencies.

The final option would be to make the control the second derivative of δ_{pc}, which would require six states and six outputs. Pitch rate and acceleration could be used as outputs (using up to the second derivative of each), so that the double integral of the control would result in measured variables and up to their double integrals. Unfortunately, the resulting C_1 matrix would be singular. Also, this would correspond to a different performance index, since we'd be penalizing the acceleration of the control deflection, and would lead to a 6-loop topology. This could be a topic of further research though the authors do not believe this will provide useful autopilot designs for missiles.

VII. Conclusions

This paper has posed and solved the classical autopilot design problem as an optimal control problem. Minimizing the performance index of acceleration error and fin deflection leads to a 2-loop autopilot topology with gains on the pitch rate and acceleration. This solution uses infinite control deflection rate to achieve a fast response. The classic 3-loop autopilot topology is a direct result of solving the weighted sum of acceleration error and fin rate. It was shown that there are multiple three loop topologies. These topologies are examined further in Mracek and Ridgely.[3]

A 4-loop "neoclassic" topology was presented. It was shown this new topology adds little complexity to the problem, but can account for additional first order dynamics directly. This 4-loop topology becomes

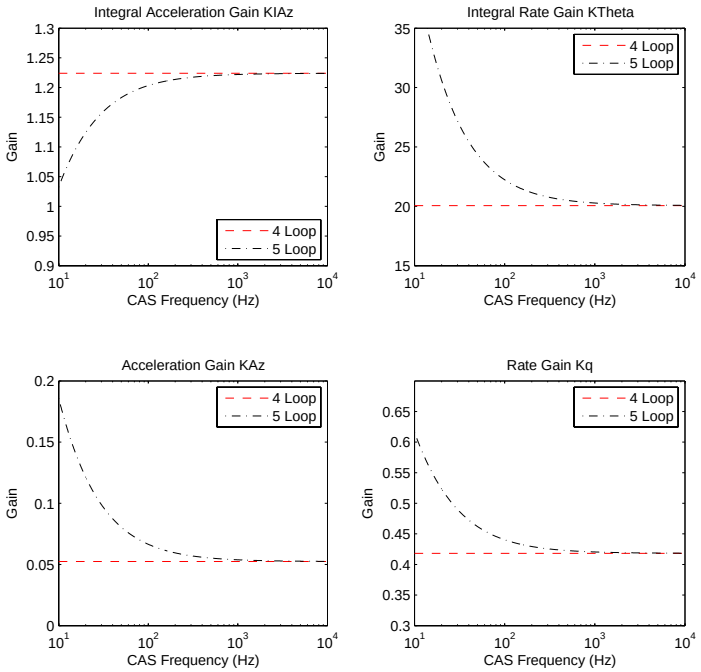

Figure 24. Gains for the 4-, and 5-Loop Systems Using $\dot{\delta}$ for feedback

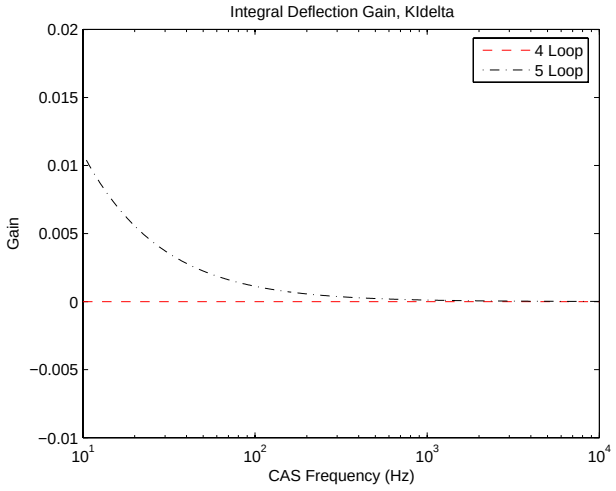

Figure 25. Gains for the 4-, and 5-Loop Systems Using $\dot{\delta}$ for feedback

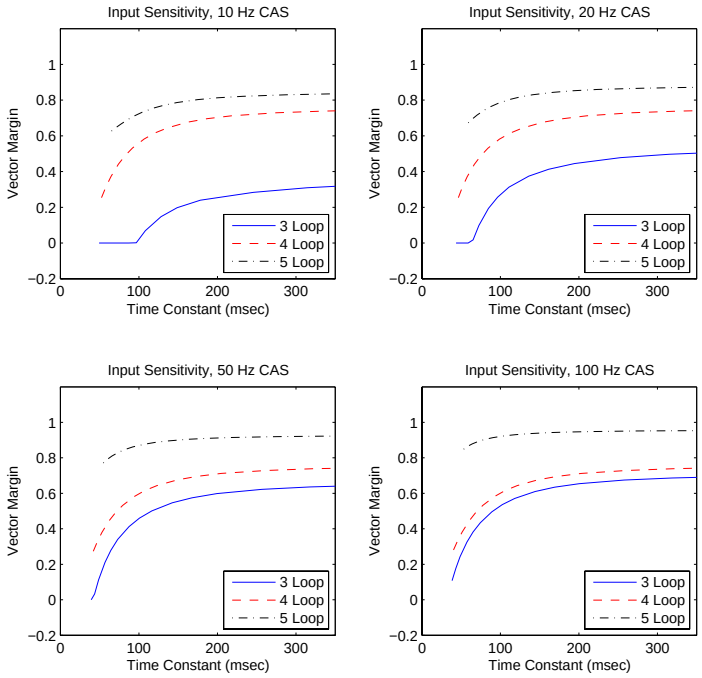

Figure 26. Vector Margins at the Plant Input for the 3-, 4-, and Alternate 5-Loop Systems with Varying CAS Frequencies

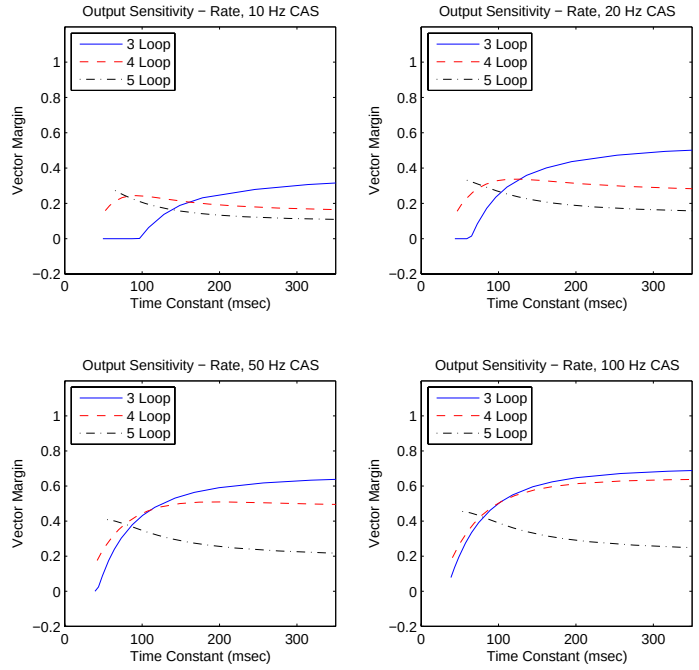

Figure 27. Vector Margins at the Rate Output for the 3-, 4-, and Alternate 5-Loop Systems with Varying CAS Frequencies

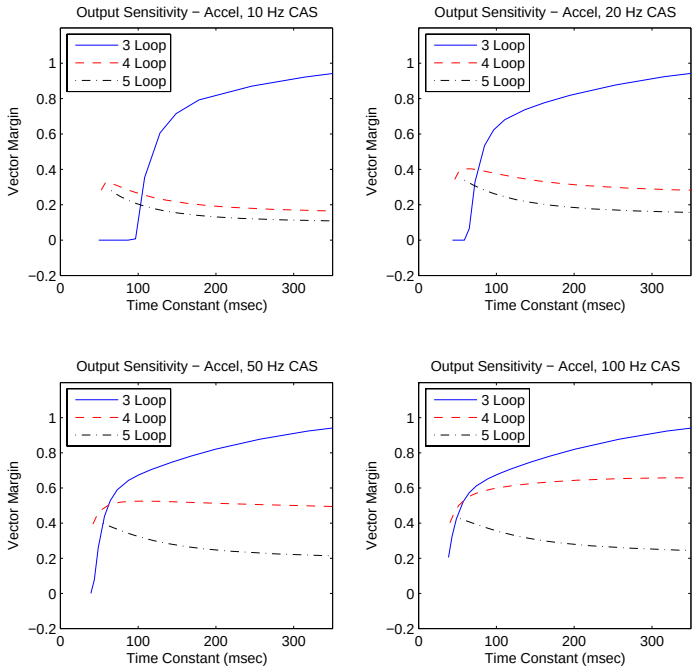

Figure 28. Vector Margins at the Acceleration Output for the 3-, 4-, and Alternate 5-Loop Systems with Varying CAS Frequencies

exactly the classic 3-loop topology as the frequency of the CAS dynamics becomes large, so it shares the same robustness properties of the classic 3-loop topology. See the follow-on paper[3] for more details on the robustness properties of the classic 3-loop topology.

Finally, two 5-loop topology that accounts for 2^{nd} order CAS dynamics directly was introduced. Unfortunately, one topology relies on feedback of δ_{pc}, which would have to be replaced with a lag filter. Thus, it does not share the robustness properties of the classic 3-loop topology. The second relies on feedback of $\dot{\delta}_{pc}$. Both 5-loop topologies result in lead compensation. Any higher order topologies either result in second or higher integrations of the acceleration command or result in the 4-loop topology with leads. The added lead continues to increase in complexity as further dynamics are added to the plant.

References

[1]Paul Zarchan, *Tactical and Strategic Missile Guidance, Fourth Edition.* AIAA Volume 199 Progress in Astronautics and Aeronautics, Reston, VA, 2002

[2]R. J. Adams and N.M. Conrardy. "Design Plant Manipulations for Implementation of an LQR Controller in a Classical Three Loop Autopilot." Technical Report, Raytheon Missile Systems, Apr. 2003

[3]C.P. Mracek and D.B. Ridgely, "Missile Longitudinal Autopilots: Comparison of Multiple Three Loop Topologies", AIAA GNC Conference, San Francisco CA, Aug. 2005

[4]F.L. Lewis and V.L. Syrmos, "Optimal Control, Second Edition", John Wiley & Sons, Inc. New York, New York, 1995